Semicond. Sci. Technol. **11** (1996) 1450–1455. Printed in the UK

Optical property simulation of single-layer halftone phaseshifting masks for DUV microlithography

Zhong-Tao Jiang†, Seungbum Hong†, Eunah Kim†, Byeong-Soo Bae†, Kwangsoo No†, Chang Kwon Hwangbo‡, Sung-Chul Lim§, Sang-Gyun Woo§ and Young-Bum Koh§

† Department of Materials Science and Engineering, Korea Advanced Institute of Science and Technology, Taejon, Korea
‡ Department of Physics, Inha University. Inchon 402-715, Korea
§ Samsung Electronics Co., Ltd, Yongin-gun, Kyongki-do, Korea

Received 15 February 1996, in final form 21 June 1996, accepted for publication 10 July 1996

Abstract. An optical simulation for a single-layer halftone phaseshifting mask (SLHTPSM) has been established and verified by the experimental data from several different sources. This simulation is suitable for a wide lithography exposure wavelength; for example, i-line, KrF and ArF etc. Theoretical analyses give some important tendencies of the optical parameters such as refractive index, extinction coefficient and film thickness. The optimum SLHTPSM structures for KrF (248 nm) have been derived by the simulation processes, which include the optimized combinations of extinction coefficient/refractive index and film thickness/refractive index achieved to deliver the 5%, 10% and 20% transmittance and 180° phaseshifting. The simulation shows the film refractive index to be in the region of 1.7–3. The simulation program also provides guidance for the SLHTPSM fabrications.

1. Introduction

At present microlithography is being developed for pattern dimensions of less than 200 nm. X-rays and e-beam projection are the potential lithography technologies in this pattern feature size region. However, it is expected that fabrications of 1 Gbit (or 4 Gbit) DRAM with a minimum feature size in the region of 200 to 150 nm will be also possible using deep-UV (DUV) optical projection lithography combined with resolution enhanced technologies, such as phaseshift masking (PSM), off-axis illumination and pupil filters. On the other hand, instead of i-line (365 nm) and KrF (248 nm) exposure light, the ArF (193 nm) excimer laser has been developed extensively for the increasing requirement of DUV-lithography [1, 2].

Mask technology is strategically important, not only for optical lithography but also for the x-ray and e-beam projection technologies, because it enables VLSI design patterns to be translated into actual fabrication. At present, improvements in masks and their fabrication technologies are becoming increasingly difficult. An alternating phaseshifting mask technique is the most effective for resolution enhancement. The phaseshifting idea in mask technology was first introduced by Levenson *et al* [3] in 1982. The conventional phaseshifting mask consists of a normal transmission mask that has been coated with a transparent layer patterned to ensure that the waves transmitted through adjacent apertures are 180° out of phase with one another; destructive interference minimizes the intensity between their images, which affects and increases the spatial resolution. A simple theory [3] predicts that any given optical system will project the images of such a phaseshifting transmission object with near doubling of resolution and higher contrast than a corresponding transmission object without phaseshifts. So this technology is very effective in improving the fine periodic line photolithography resolution. Furthermore, application of this technology to improve the resolution of isolated patterns has also been investigated [4–7].

Terasawa *et al* [7] summarized the conventional phaseshifting masks, which can be roughly classified into two types: (i) a frequency-doubling mask with phaseshifting apertures placed alternately in periodic patterns and (ii) an edge-enhancement mask with very small phaseshifted regions around the main apertures. A halftone phaseshifting mask, a new type of phaseshifting mask which is similar to the additional apertures of edge-enhancement masks, has been developed since the early 1990s. A halftone phaseshifting mask consists of a transparent substrate, such as quartz, and an attenuated halftone layer with an optical transmittance between 5 and 20%. The halftone mask regions are also phaseshifted

0268-1242/96/101450+06$19.50

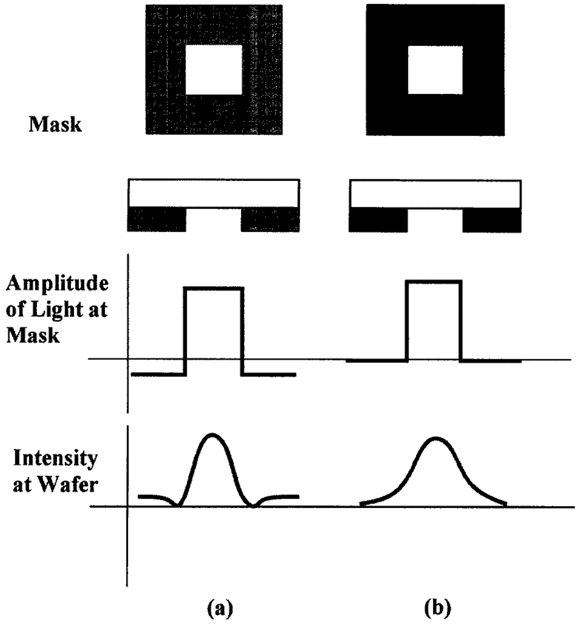

Figure 1. Schematic diagrams of structure and transmitted light intensities: (*a*) a halftone-shifting mask and (*b*) a conventional transmission mask.

by 180° with respect to the apertures, which plays a role in reducing the size of bright feature (see the schematic diagram in figure 1). The weak light passes through the halftone region, but its intensity is insufficient to develop the photoresist on the wafer. The halftone phaseshifting is one of the most practical methods because (i) the mask structure is simple, (ii) mask fabrication is relatively easy and (iii) the design of existing steppers need not be modified. Further investigations [7, 8] revealed that the halftone phaseshifting mask has a better performance than other conventional transmission masks on the basis of both theory and experiment. By using this technology, a mask design with intermediate transmittance values is effective for fabricating isolated hole patterns because it does not require a special layout design. Overall, a halftone phaseshifting mask has two basic features, namely transmittance limitation and 180° phaseshifting.

In the early stage, the phaseshifting mask has two (or more) layers taking responsibility for transmittance control and phaseshifting control respectively. A conventional double-layer mask, however, could suffer structural drawbacks (such as many pinhole defects) and difficulties in the etching process, especially in the DUV exposure region. Since 1993, the single-layer (monolayer) halftone phaseshifting mask (SLHTPSM) has been investigated and developed extensively. A number of thin film materials have been fabricated and characterized, such as CrO, CrN, CrON, CrOCN, CrF, SiNx, SiO_2–CrO, MoSiO, MoSiON and W/Si films [8–13]. In SLHTPSM, the single-layer mask film plays the role of controlling both transmittance and phaseshifting. Proper combinations of refractive index and extinction coefficient can be achieved to deliver the required transmittance and phaseshifting at reasonable film thicknesses by changing the mixing ratio of two selected materials (or the composition of the films) and deposition parameters. In this circumstance, the system simulation is extremely important and helpful for finding suitable combinations of the optical properties. In 1994, Ito and co-workers [14] reported the optimum optical properties of a single-layer halftone mask and provided some optimum conditions for the refractive index (n), extinction coefficient (k) and film thickness (d) of SLHTPSM for i-line (365 nm) exposure wavelength and 5% transmittance.

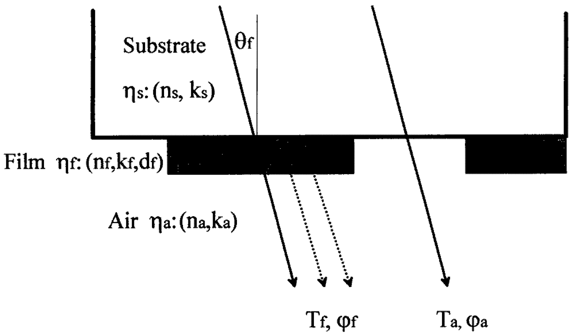

Figure 2. The physical model of the non-multireflection effect (solid lines) and multireflection effect (solid + dotted lines) in SLHTPSM.

In the present paper, we will expand the optical simulation work for SLHTPSM from i-line to KrF, or lower wavelength. Some necessary verifications for the simulation will be carried out. Theoretical analyses based on this simulation reveal the optimum relationships among the various optical parameters of SLHTPSM in the DUV exposure region and predict some important tendencies of these parameters; they also provide guidance for the SLHTPSM fabrications.

2. Optical simulation for SLHTPSM

2.1. Physical model

The PSM film is deposited on a transparent substrate, such as quartz, and subsequently written by a line and space pattern [7, 8, 14], so that the physical model for the SLHTPSM can be designed as shown in figure 2. The basic requirements for this system are: (i) $T_{PSM} = T_f/T_a = 5\%$ (or up to 20%); and (ii) $\varphi_{PSM} = \varphi_f - \varphi_a = 180°$. The optical parameters: (n_s, k_s), (n_f, k_f), and (n_a, k_a), are for the substrate, single-layer phaseshifting film and air respectively. d_f is the thickness of the single-layer phaseshifting film. The substrate is considered as a semi-infinite medium.

A preliminary study of non-multireflection analysis will give us some indications for undertaking more precise optical analysis. In the case of non-multireflection, the phase change of the film part and the non-film part can be described as follows:

$$\varphi_f = \frac{2\pi n_f d_f}{\lambda} \tag{1}$$

and

$$\varphi_a = \frac{2\pi d_f}{\lambda} \tag{2}$$

where λ is the wavelength of the exposure light. Due to the relative phaseshift, ϕ_{PSM} is required to be 180°, and the first relationship can be derived from equations (1) and (2).

$$d_{\mathrm{f}} = \frac{\lambda}{2(n_{\mathrm{f}} - 1)}. \tag{3}$$

The extinction coefficient governs the decay of the wave as it propagates through the material, so that the irradiance and the transmittance (T) are given by

$$I(d) = I(0)\exp[-(4\pi k d/\lambda)]$$

and

$$T = I(d)/I(0) \tag{4}$$

respectively, where k is k_{f} (or k_{a}) and d is d_{f} (or d_{a}). The extinction coefficient (k_{f}) can be written as

$$k_{\mathrm{f}} = -\frac{\lambda \ln(T')}{4\pi d_{\mathrm{f}}} \tag{5}$$

where $T' = T_{\mathrm{f}}/T_{\mathrm{a}}$ is the relative transmittance of the PSM system, while k_{a} is zero and $d_{\mathrm{a}} = d_{\mathrm{f}}$.

Equations (3) and (5) are the basic relationships of the optical parameters for the PSM under the non-multireflection condition, which are derived from the phaseshifting and attenuation requirements respectively.

2.2. Matrix approach

A more precise theoretical analysis should consider the multireflection effect of the mask film. The alternative matrix approach of Fresnel coefficients uses Maxwell's equations and properties of optical impedance and admittance. Impedance varies continuously through a thin film even though there is a refractive index discontinuity at film boundaries. By equating the tangential components of the electric and magnetic field vectors on both sides of a film boundary and by expressing the change in the admittance as a function of layer depth, even the most complex thin film structure can be represented in a compact form that is suitable for highly efficient simulation programming.

Full derivations of the matrix formulation have been presented in numerous publications, the better treatments, however, are included in [15] and [16]. A further development of the matrix theory for a multilayer thin film system was carried out to derive a matrix formulation which is suitable for the SLHTPSM system as described in figure 2 [14, 16]. The amplitude of transmission coefficients is given by

$$t = \frac{2\eta_{\mathrm{s}}}{\eta_{\mathrm{s}} B + C} = \alpha + \mathrm{i}\beta \tag{6}$$

where

$$\begin{bmatrix} B \\ C \end{bmatrix} = \begin{bmatrix} E_{\mathrm{s}} \\ H_{\mathrm{s}} \end{bmatrix} = M_{\mathrm{f}} \begin{bmatrix} 1 \\ \eta_{\mathrm{a}} \end{bmatrix}. \tag{7}$$

E_{s} and H_{s} are the electric and magnetic vectors, respectively, in the incident medium (substrate here) and M_{f} is a 2 × 2 product matrix which represents the single-layer PSM film of the system

$$M_{\mathrm{f}} = \begin{bmatrix} \cos\delta_{\mathrm{f}} & \frac{\mathrm{i}}{\eta_{\mathrm{f}}}\sin\delta_{\mathrm{f}} \\ \mathrm{i}\eta_{\mathrm{f}}\sin\delta_{\mathrm{f}} & \cos\delta_{\mathrm{f}} \end{bmatrix} \tag{8}$$

where

$$\delta_{\mathrm{f}} = \frac{2\pi}{\lambda}(\eta_{\mathrm{f}} d_{\mathrm{f}} \cos\vartheta_{\mathrm{f}}) \tag{9}$$

and

$$\eta_{\mathrm{s}} = n_{\mathrm{s}}$$
$$\eta_{\mathrm{f}} = n_{\mathrm{f}} - \mathrm{i}k_{\mathrm{f}} \tag{10}$$
$$\eta_{\mathrm{a}} = n_{\mathrm{a}}.$$

η is often called the complex refractive index. The intensity transmittances through the film part and space part are given by

$$T_{\mathrm{f}} = \frac{\eta_{\mathrm{a}}}{\eta_{\mathrm{s}}}|t_{\mathrm{f}}|^2 = \frac{n_{\mathrm{a}}}{n_{\mathrm{s}}}(\alpha_{\mathrm{f}}^2 + \beta_{\mathrm{f}}^2) \tag{11a}$$

and

$$T_{\mathrm{a}} = \frac{\eta_{\mathrm{a}}}{\eta_{\mathrm{s}}}|t_{\mathrm{a}}|^2 = \frac{n_{\mathrm{a}}}{n_{\mathrm{s}}}(\alpha_{\mathrm{a}}^2 + \beta_{\mathrm{a}}^2) \tag{11b}$$

respectively. The relative transmittance (in %) of SLHTPSM is

$$T_{\mathrm{PSM}} = \frac{T_{\mathrm{f}}}{T_{\mathrm{a}}}. \tag{12}$$

The phase changes of transmission regarding the film part and the air part are described as follows:

$$\varphi_{\mathrm{f}} = \arctan(\beta_r/\alpha_r) \tag{13a}$$

and

$$\varphi_{\mathrm{a}} = \arctan(\beta_{\mathrm{a}}/\alpha_{\mathrm{a}}) \tag{13b}$$

so that the phaseshift of the SLHTPSM, i.e. the relative phaseshift between the film part and the air part, is given by

$$\varphi_{\mathrm{PSM}} = \varphi_{\mathrm{f}} - \varphi_{\mathrm{a}}. \tag{14}$$

Equations (12) and (14) give the calculated transmittance and phaseshifting under the given optical parameters of the SLHTPSM. Starting from equations (3) and (5) which provide the initial values of k_{f} and d_{f} for a certain refractive index (n_{f}) and optimum transmittance and phaseshifting, for example $T'_{\mathrm{PSM}} = 5\%$ and $\varphi'_{\mathrm{PSM}} = 180°$, the simulation program based on the matrix approach calculates the T_{PSM} and φ_{PSM} values of the SLHTPSM. By changing the d_{f} and k_{f} values, the transmittance error $T'_{\mathrm{PSM}} - T_{\mathrm{PSM}}$ and phaseshifting error $\varphi'_{\mathrm{PSM}} - \varphi_{\mathrm{PSM}}$ approach zero. Then the optimized combination of $n_{\mathrm{f}}, k_{\mathrm{f}}$ and d_{f} of a given system are achieved. A simulation program based on the theory has been developed.

3. Results and discussion

3.1. System simulation verifications

In 1994, Mohri and co-workers [8] reported their experimental results regarding a chromium fluoride single-layer film/quartz plate for a 250 nm exposure wavelength. The optical parameters of their fabricated PSM film were $n_{\mathrm{f}} = 1.68$, $k_{\mathrm{f}} = 0.19$ and $d_{\mathrm{f}} = 185$ nm. The optical transmission spectrum obtained by a spectroscopic ellipsometer indicates that the transmittance is about 16% at 250 nm wavelength with 180° phaseshifting. Using Mohri *et al*'s data (i.e. n, k and d), our simulation program

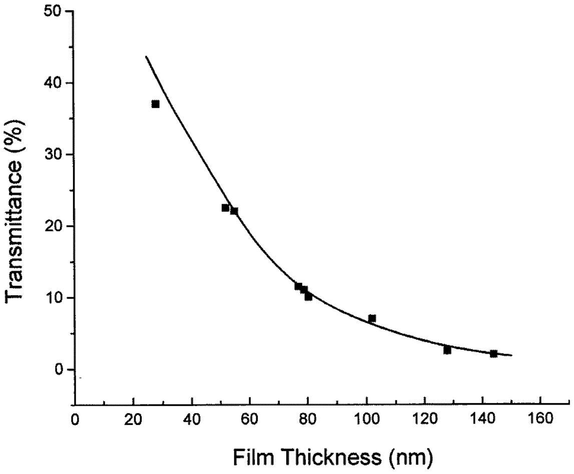

Figure 3. The film thickness dependence of the optical transmittance at 248 nm: full curve, simulation results, full squares, results of O'Grady and Wilber [17].

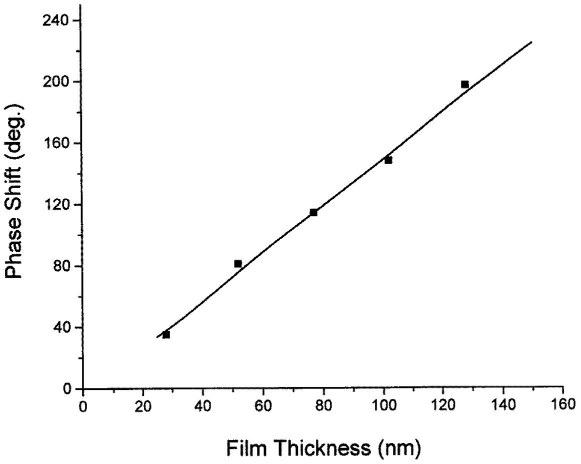

Figure 4. The film thickness dependence of the phaseshift at 248 nm: full line, simulation results; full squares, results of O'Grady and Wilber [17].

confirms that the transmittance and phaseshifting of this system are 16.5% and 180.1°, respectively.

O'Grady and Wilber [17] provided the details of the thermal oxidation processed single-layer chrome film on a 5″ 90 mil quartz substrate. In their publication, they gave the variations of optical transmission and phaseshifting according to the different film thicknesses at exposure wavelengths of 248 and 365 nm. Figures 3 and 4 show simulation results (full curve) and O'Grady and Wilber's results of the transmittance and phaseshifting at 248 nm wavelength respectively. Through the optimum process, the refraction index (n_f) and extinction coefficient (k_f) for the best fit of both transmittance and phaseshifting experimental results are 2.05 and 0.52 respectively. The k_f value obtained by this simulation process is located in the normal region, but the n_f value seems slightly smaller than that from [11] (i.e. the typical range of n_f for CrO is about 2.2–2.6). The results from experiment and simulation are correlated very well for both transmittance and phaseshifting, except for the transmittance value in the film thickness range below 50 nm. This might be due to the fact that the thermal oxidation process affects the construction of the interface layer between the pure chrome film and the substrate; this might change the transparency of the film and the accuracy of film thickness measurement. The thicker chrome thin film could limit the oxidation rate of the chrome film and affect the interface layer less. A further comparison shows the simulation process to be well correlated with the characterization of some other real mask films [18]. Table 1 lists both experimental results and simulation results for these masks.

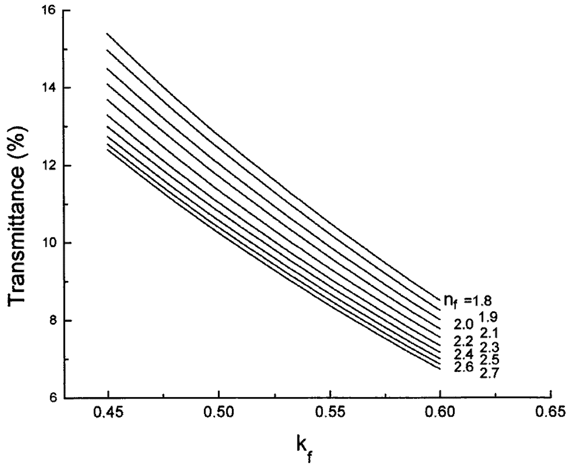

Figure 5. The film extinction coefficient (k_f) dependence of the optical transmittance with different refractive indices (n_f) from 1.8 to 2.7 at 248 nm, where the film thickness (d_f) is 80 nm and the refractive index of the substrate is 1.507.

3.2. Theoretical analyses and the optimized SLHTPSM structure for DUV lithography

A theoretical analysis based on the simulation will give us some idea of the quantitative relationships among the parameters of n_f, k_f, d_f, T, phaseshifting and the incident light wavelength (λ). In the case of a given wavelength and film thickness, the variation of the k_f value strongly affects the transmittance but only weakly affects the phaseshifting while n_f remains constant. Figures 5 and 6 are the plots of simulation results which indicate that, for a given n_f value, a 10% margin tolerance of k_f value will lead to about 20% tolerance for the transmittance and only about 0.5% shifting for the phase changing. However, the changing of the n_f value, while keeping the k_f value constant, will cause a relatively small transmittance change but a large phaseshifting. A variation of 5% in the n_f value causes about a 3% change for transmittance (figure 5) and about 10% shifting for phase-changing (figure 6). So we may conclude that the n_f and k_f values mainly dominate the phaseshifting and transmittance, respectively, of an attenuated phaseshifting film under a certain wavelength and film thickness.

The physical model and simulation program developed

Table 1. Comparison of some real SLHTPSM experimental results and simulation results at 248 nm.

Sample	d_f (nm) for $\varphi = 180°$ (expt.)	n_f (expt.)	k_f (expt.)	T (expt.) (%)	T (calc.) (%)	φ (calc.) (deg)
Ta/LNO 25W/50W	136.3	1.91	0.382	6.1	6.6	181.3
Ta/LNO 35W/80W	151.2	1.82	0.415	3.7	3.9	181.6
Ta/LNO 40W/50W	118.3	2.05	0.312	13	14	180.6

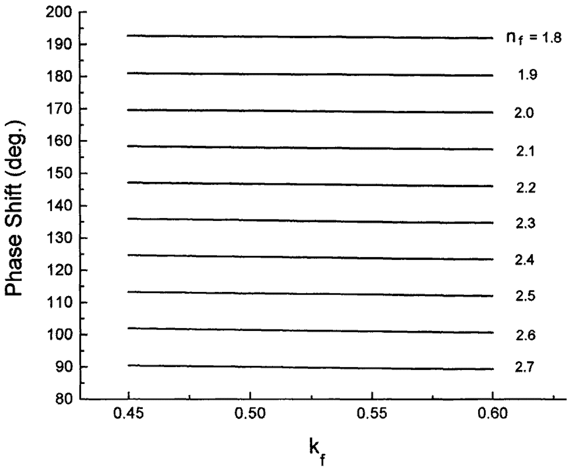

Figure 6. The film extinction coefficient (k_f) dependence of the phaseshift with different refractive indices (n_f) from 1.8 to 2.7 at 248 nm, where the film thickness (d_f) is 80 nm and the refractive index of the substrate is 1.507.

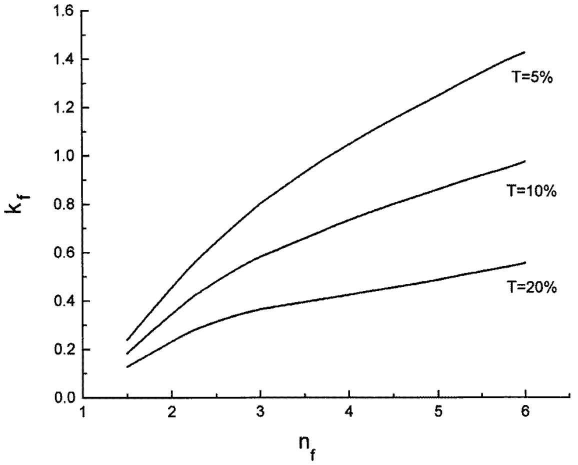

Figure 7. The optimized combinations of extinction coefficient (k_f) and refractive index (n_f) for transmittances of 5%, 10% and 20%, and a phaseshifting of 180(±0.5%)° at 248 nm, where the corresponding film thicknesses are given by figure 8 and the refractive index of the substrate is 1.507.

above can optimize the SLHTPSM film structure for microlithography (or even for a shorter exposure wavelength, for example 193 nm of ArF) without much difficulty. Here, we present the optimum single-layer halftone phaseshifting mask structure for DUV photolithography. Figure 7 shows the relationship between k_f and n_f parameters for 248 nm exposure light. These optimized n_f and k_f values match the requirements of halftone phaseshift masks, i.e. $\varphi_{PSM} = 180°$ and $T = 5\%$, 10% and 20%. The optimum tolerance is less than 2% and 0.5% for transmittance and phaseshifting respectively. A further analysis indicates that a 1% of margin tolerance for the thickness (d_f) of the attenuated film will create about a 2.5% difference for transmittance and about a 1% difference for phaseshifting under the given λ, n_f and k_f values. The film transmittance, in the case of SLHTPSM, can be mainly adjusted by the extinction coefficient (k_f) because the film thickness is restricted by the 180° phaseshifting requirement. Figure 8 shows the optimized mask film thickness calculated for various refractive index values for the 248 nm exposure light and 180(±0.5%)° phaseshift, where the transmittances are 5%, 10% and 20%. Figure 8 clearly shows that at refractive index (n_f) values < 2.5 transmittance variations in the range 5–20% have no effect on optimized mask thickness (d_f), and at values above this, between 2.5 and 6, that there is slight dispersion which is just a broadening of the line. Simulation processes also indicate, within a wide range of exposure wavelengths, that the margin of tolerance of film thickness has a similar effect to the transmittance and phaseshifting over the considerable refractive index range. The higher refractive index value, however, needs a smaller film thickness to match the target requirements; this would cause more difficulties in controlling the accuracy of the film thickness during fabrication, so that high-refractive-index film materials (for example $n > 3$) are not feasible candidates for SLHTPSM in DUV region lithography (or lower).

4. Conclusions

A physical model and simulation program for SLHTPSM have been established. This system has been verified by experimental data from several different sources. Theoretical analyses indicate that, for a given λ and film thickness (d_f), the transmittance and phaseshifting are mainly controlled by the extinction coefficient (k_f) and refractive index (n_f), as well as being weakly affected by the refractive index and extinction coefficient, respectively, of the attenuated film. The optimum SLHTPSM structures have been derived by the simulation processes. The optimized combination of extinction coefficient/refractive index and film thickness/refractive index have been achieved to deliver the 5%, 10% and 20% transmittance and 180° phaseshifting for 248 nm exposure wavelength single-layer halftone phaseshifting masks. A further analysis gives a reasonable refractive index value for SLHTPSM

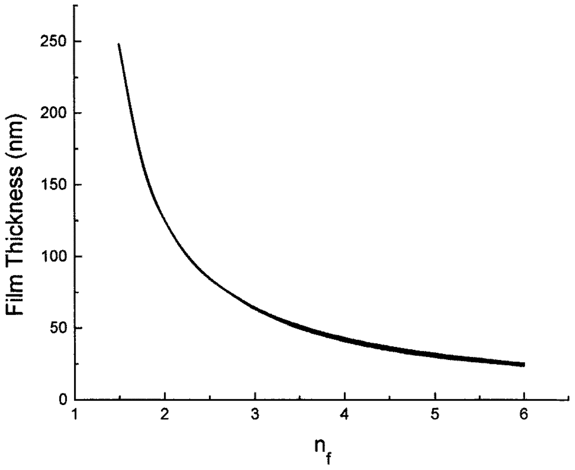

Figure 8. The optimized combinations of film thickness (d_f) and refractive index (n_f) for transmittances of 5%, 10%, and 20% and a phaseshifting of 180(±0.5%)° at 248 nm, where the corresponding extinction coefficient (k_f) is given by figure 7 and the refractive index of the substrate is 1.507.

in the region of 1.7–3. Mask materials with a higher refractive index cause more difficulties in fabricating good quality phaseshifting masks. This simulation program also provides guidance for SLHTPSM fabrication.

Acknowledgments

The authors would like to express their gratitude to Mr I G Yoo and Mr H G Cho of the Physics Department at Inha University for their help in running the Essential Macleod Thin Film Design Software to verify the basic part of this simulation.

References

[1] Endert H, Patzel R, Rebhan U, Powell M and Basting D 1995 New KrF and ArF excimer lasers for advanced deep ultraviolet optical lithography *Japan. J. Appl. Phys.* **34** 4050

[2] Hibbs M, Kunz R and Rothschild M 1995 193 nm lithography at MIT Lincoln Lab *Semicond. Sci. Technol.* July 69

[3] Levenson M D, Viswanathan N S and Simpson R A 1982 Improving resolution in photolithography with a phase-shifting mask *IEEE Trans. Electron Devices* **29** 1828

[4] Terasawa T, Hasegawa N, Kurosaki T and Tanaka T 1989 0.3-micron optical lithography using a phaseshifting mask *SPIE Proc.* **1088** 25

[5] Hashimoto K, Samuels D J, Farrell T R, Moy D, Martino R M, Ferguson R A, Sato T and Maurer W 1994 The application of deep UV phase shifted-single layer halftone reticles to 256 Mbit dynamic random access memory cell patterns *Japan. J. Appl. Phys.* **33** 6823

[6] Otaka A, Kawai Y and Matsuda T 1993 Hole pattern fabrication using halftone phase-shifting masks in KrF lithography *Japan. J. Appl. Phys.* **32** 5880

[7] Terasawa T, Hasegawa N, Fukuda H and Katagiri S 1991 Imaging characteristics of multi-phase-shifting and halftone phase-shifting masks *Japan. J. Appl. Phys.* **30** 2991 and its refs.[4] and [8]

[8] Mohri H, Takahashi M, Mikami K, Miyashita H, Hayashi N and Sano H 1994 Chromium-based attenuated phase shifter for DUV exposure *SPIE Proc.* **2322** 288; 1994 Manufacturing of half-tone phaseshift masks I. Blank, II. Writing and process and III. Inspection, repair and quality assurance *SPIE Proc.* **2254** 238

[9] Iwabuchi Y, Ushioda J, Tanabe H, Ogura Y and Kishida S 1993 Monolayer halftone phase-shifting mask for KrF excimer laser lithography *Japan. J. Appl. Phys.* **32** 5900

[10] Kawano K, Asano M, Tanaka S, Iwamatsu T, Sato H and Ito S I 1995 Lithography performance of SiNx single-layer halftone mask *SPIE Proc.* **2512** 348

[11] Nakajima M, Yoshioka N, Miyazaki J, Kusunose H, Hosono K, Morimoto H, Wakamiya W, Murayama K, Watakabe Y and Tsukamoto K 1994 Attenuated phaseshifting mask with a single-layer absorptive shifter of CrO, CrON, MoSiO and MoSiON film *SPIE Proc.* **2197** 111

[12] Mitsui H, Sakai H and Yamaguchi Y 1995 Development of the W/Si film for the single-layered attenuated phase shifting mask for 248nm lithography *SPIE Proc.* **2512** 343

[13] Simth B W and Butt S 1995 Attenuating phase-shift masks for 193nm *First Int. Symp. on 193nm Lithography (Colorado Springs, Colorado, 15–18 August 1995) Digest of Abstracts* p 89

[14] Ito S I, Hazama H, Kamo T, Miyazaki H, Sato H, Hayashi K, Shigemitsu H and Mori I 1994 Optimization of optical properties for single-layer halftone masks *SPIE Proc.* **2197** 99

[15] Macleod H A 1986 *Thin-film Optical Filters* 2nd edn (Bristol: Adam Hilger) ch 2

[16] Dobrowolski J A 1995 *Handbook of Optics* vol 2 Editor in Chief M Bass (New York: McGraw-Hill) ch 42

[17] O'Grady D S and Wilber P B 1994 Attenuating phase-shift mask by thermal oxidation of chrome *SPIE Proc.* **2197** 194

[18] Cheng C-C, Wu T B, Gan J-Y, Tuo L C and Wang J J 1996 $(\mathrm{LaNiO_3})_x(\mathrm{Ta_2O_5})_{1-x}$ oxide thin films for attenuated phase-shifting mask blank *Photomask Japan '96 (Symp. on Photomask and X-Ray Mask Technology III, Kanagawa, Japan, 18–19 April 1996) Digest of Papers* p 48